ESI

Slow relaxations of Dy(III) single-ion magnets dominated by simultaneous binding of chelating ligands in low-symmetry ligand-fields

Hui-Ming Dong,[a,b] Zhong-Yi Liu,[a] Hui-Min Tang,[a] En-Cui Yang,*[a] Yi-Quan Zhang*[c] and Xiao-Jun Zhao[a,b]

[a] *College of Chemistry, Tianjin Key Laboratory of Structure and Performance for Functional Molecules, Tianjin Normal University, Tianjin 300387, People's Republic of China*

[b] *Department of Chemistry, Collaborative Innovation Center of Chemical Science and Engineering, Nankai University, Tianjin 300071, People's Republic of China.*

[c] *Jiangsu Key Lab for NSLSCS, School of Physical Science and Technology, Nanjing Normal University, Nanjing 210023, China*

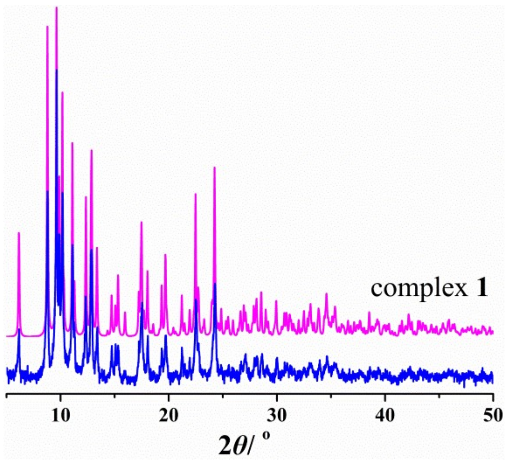

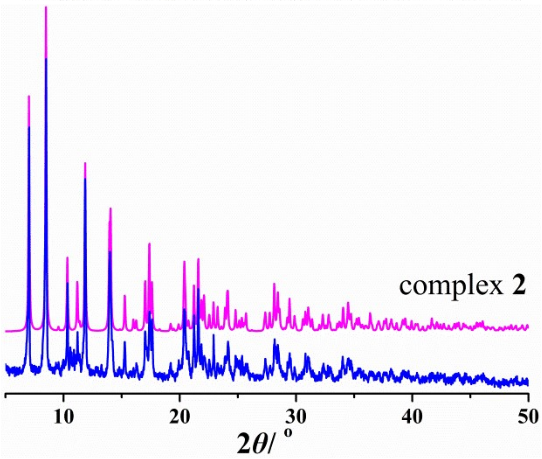

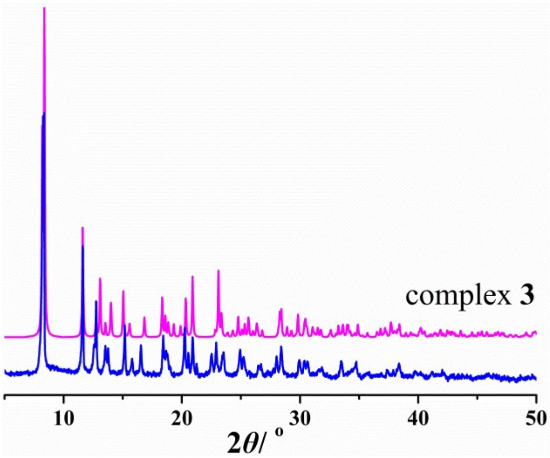

Fig. S1. Simulated (purple) and experimental (blue) PXRD patterns for **1** – **3**.

Table S1. Crystal and structure refinement data for **1–3** [a]

	1	**2**	**3**
empirical formula	$C_{31}H_{26}DyN_5O_6$	$C_{46}H_{39}ClDyN_7O_7$	$C_{38}H_{28}DyN_7O_7$
F_w	727.07	999.79	857.17
cryst size [mm]	0.22× 0.21× 0.18	0.22 × 0.21 × 0.18	0.22 × 0.21 × 0.18
cryst syst	triclinic	monoclinic	monoclinic
space group	$P\bar{1}$	$P2_1/c$	$C2/c$
a [Å]	10.249(2)	13.5337(19)	14.948(3)
b [Å]	10.840(3)	18.459(3)	19.059(4)
c [Å]	14.915(3)	18.405(2)	14.435(4)
α [º]	90.353(5)	90	90
β [º]	105.031(5)	111.693(9)	119.103(3)
γ [º]	111.198(4)	90	90
V [Å^3]	1482.8(6)	4272.3(11)	3593.2(14)
Z, D_c [g cm^{-3}]	2, 1.628	4, 1.554	4, 1.584
h / k / l	–12, 11/–13, 12/–12, 18	–16, 16/–22, 23/–23, 22	–18, 18/–10, 23/–18, 17
F(000)	722	2012	1708
μ [mm^{-1}]	2.572	1.872	2.139
reflections collected / unique	19742 / 6372	24592 / 8817	10301 / 3721
R_{int}	0.0284	0.0324	0.0296
data / restraints / params	6132 / 0 / 391	8814 / 12 / 560	3721 / 66 / 259
R_1^a, wR_2^b [$I > 2\sigma(I)$]	0.0373, 0.0706	0.0238, 0.0607	0.0331, 0.0979
R_1, wR_2 [all data]	0.0489, 0.0746	0.0323, 0.0637	0.0392, 0.1008
GOF on F^2	1.008	1.039	1.061
$\Delta\rho_{max}$, $\Delta\rho_{min}$ [e·Å^{-3}]	1.609, –0.791	0.76, –0.48	1.040, –0.604

[a] $R_1 = \Sigma(||F_o|-|F_c||)/\Sigma|F_o|$; [b] $wR_2 = [\Sigma w(|F_o|^2-|F_c|^2)^2/\Sigma w(F_o^2)^2]^{1/2}$.

Table S2. Calculation of the agreement between the coordination polyhedron of the studied complexes with various ideal polyhedra using the SHAPE program*

SIM	CShM		
	SAP (D_{4d})	TDD (D_{2d})	BTPR (C_{2v})
1	2.160	1.361	2.257
2	1.472	1.569	2.593
3	1.482	1.376	2.678

* SAP = Square antiprism, TDD = Triangular dodecahedron and BTPR= Biaugmented trigonal prism

Table S3. Selected bond lengths (Å) and angles (deg) for **1**

Dy(1)–O(3)	2.178(3)	Dy(1)–O(1)	2.269(3)
Dy(1)–O(5)	2.293(2)	Dy(1)–N(1)	2.492(4)
Dy(1)–N(3)	2.521(3)	Dy(1)–N(4)	2.552(3)
Dy(1)–N(2)	2.570(3)	Dy(1)–N(5)	2.574(4)
O(3)–Dy(1)–O(1)	85.44(11)	O(3)–Dy(1)–O(5)	140.57(10)
O(1)–Dy(1)–O(5)	122.35(11)	O(3)–Dy(1)–N(1)	92.57(12)
O(1)–Dy(1)–N(1)	69.79(11)	O(5)–Dy(1)–N(1)	74.78(11)
O(3)–Dy(1)–N(3)	149.50(10)	O(1)–Dy(1)–N(3)	71.65(10)
O(5)–Dy(1)–N(3)	69.93(10)	N(1)–Dy(1)–N(3)	97.86(12)
O(3)–Dy(1)–N(4)	78.62(11)	O(1)–Dy(1)–N(4)	76.84(11)
O(5)–Dy(1)–N(4)	131.05(11)	N(1)–Dy(1)–N(4)	146.07(12)
N(3)–Dy(1)–N(4)	76.78(11)	O(3)–Dy(1)–N(2)	69.49(10)
O(1)–Dy(1)–N(2)	137.98(11)	O(5)–Dy(1)–N(2)	71.36(9)
N(1)–Dy(1)–N(2)	77.98(12)	N(3)–Dy(1)–N(2)	140.74(10)
N(4)–Dy(1)–N(2)	126.96(12)	O(3)–Dy(1)–N(5)	102.40(12)
O(1)–Dy(1)–N(5)	135.70(11)	O(5)–Dy(1)–N(5)	77.75(11)
N(1)–Dy(1)–N(5)	150.72(11)	N(3)–Dy(1)–N(5)	81.90(11)
N(4)–Dy(1)–N(5)	62.64(11)	N(2)–Dy(1)–N(5)	83.86(11)

Table S4. Natural bond order (NBO) charges on each donor for the ground state of **1**–**3** obtained by CASSCF calculation

Donors in **1**	charge	Donors in **2**	charge	Donors in **3**	charge
O5	–0.895	O1	–0.921	O1A	–0.925
N1	–0.212	N1	–0.228	N1A	–0.229
N2	–0.217	N3	–0.375	N2A	–0.377
N5	–0.362	N5	–0.383	N3	–0.379
N3	–0.206	N2	–0.236	N1	–0.229
O1	–0.890	O2	–0.910	O1	–0.925
O3	–0.896	N4	–0.381	N3A	–0.379
N4	–0.345	N6	–0.376	N2	–0.377

Table S5. Selected bond lengths (Å) and angles (deg) for **2**

Dy(1)–O(1)	2.223(16)	Dy(1)–O(2)	2.2372(16)
Dy(1)–N(1)	2.491(2)	Dy(1)–N(2)	2.499(2)
Dy(1)–N(3)	2.543(2)	Dy(1)–N(6)	2.546(2)
Dy(1)–N(5)	2.558(2)	Dy(1)–N(4)	2.563(2)
O(1)–Dy(1)–O(2)	134.86(7)	O(1)–Dy(1)–N(1)	70.58(6)
O(2)–Dy(1)–N(1)	75.15(6)	O(1)–Dy(1)–N(2)	75.34(6)
O(2)–Dy(1)–N(2)	70.09(6)	N(1)–Dy(1)–N(2)	79.26(9)
O(1)–Dy(1)–N(3)	75.97(6)	O(2)–Dy(1)–N(3)	142.23(6)
N(1)–Dy(1)–N(3)	104.77(7)	N(2)–Dy(1)–N(3)	147.67(6)
O(1)–Dy(1)–N(6)	142.27(6)	O(2)–Dy(1)–N(6)	76.50(7)
N(1)–Dy(1)–N(6)	147.13(7)	N(2)–Dy(1)–N(6)	106.18(7)
N(3)–Dy(1)–N(6)	87.85(7)	O(1)–Dy(1)–N(5)	79.45(7)
O(2)–Dy(1)–N(5)	120.87(6)	N(1)–Dy(1)–N(5)	147.10(7)
N(2)–Dy(1)–N(5)	80.32(7)	N(3)–Dy(1)–N(5)	80.07(6)
N(6)–Dy(1)–N(5)	64.13(7)	O(1)–Dy(1)–N(4)	120.15(6)
O(2)–Dy(1)–N(4)	79.22(7)	N(1)–Dy(1)–N(4)	78.32(7)
N(2)–Dy(1)–N(4)	145.67(7)	N(3)–Dy(1)–N(4)	64.23(7)
N(6)–Dy(1)–N(4)	80.36(7)	N(5)–Dy(1)–N(4)	130.28(8)

Table S6. Selected bond lengths (Å) and angles (deg) for **3** [a]

Dy(1)–O(1)	2.221(3)	Dy(1)–N(3)	2.546(4)
Dy(1)–N(1)	2.488(4)	Dy(1)–N(2)	2.547(4)
O(1)–Dy(1)–N(1)$^{\#1}$	74.26(12)	O(1)–Dy(1)–O(1)$^{\#1}$	132.66(16)
O(1)–Dy(1)–N(3)	80.10(12)	O(1)–Dy(1)–N(1)	70.57(12)
N(1)$^{\#1}$–Dy(1)–N(3)	81.98(13)	N(1)$^{\#1}$–Dy(1)–N(1)	82.42(19)
O(1)–Dy(1)–N(2)$^{\#1}$	79.15(12)	O(1)$^{\#1}$–Dy(1)–N(3)	123.89(12)
N(1)–Dy(1)–N(2)	146.09(12)	N(1)–Dy(1)–N(3)	149.57(13)
N(3)–Dy(1)–N(2)$^{\#1}$	72.96(13)	N(3)–Dy(1)–N(3)$^{\#1}$	122.58(18)
N(3)–Dy(1)–N(2)	64.13(12)	O(1)–Dy(1)–N(2)	142.92(12)
N(2)$^{\#1}$–Dy(1)–N(2)	81.23(18)	N(1)–Dy(1)–N(2)$^{\#1}$	108.19(13)

[a] Symmetry codes: $^{\#1}$ $-x$, y, $1/2-z$.

Table S7. Hydrogen-bonding parameters (Å, deg) in **1**–**3** [a]

D–H···A	*d* (D–H)	*d* (H···A)	*d* (D···A)	∠DHA
1				
O(2)–H(2)···O(4)[#1]	0.820	2.381	2.893	121.33
C(14)–H(14)···O(6)[#2]	0.930	2.544	3.435	160.63
2				
C(21)–H(21)···O(4)[#1]	0.930	2.417	3.221	144.74
C(27)–H(27)···O(3)[#2]	0.930	2.578	3.355	141.37
3				
C(14)–H(14)···O(2)[#1]	0.930	2.349	3.172	147.42

[*] Symmetry codes for **1**: [#1]$1 - x$, $1 - y$, $1 - z$; [#2] $x + 1$, y, z. For **2**: [#1]$1 - x$, $1 - y$, $1 - z$; [#2] $-x$, $1 - y$, $1 - z$; [#3]$x - 1$, y, z; [#4]x, $1/2 - y$, $z + 1/2$. For **3**: [#1]x, $1 - y$, $z - 1/2$.

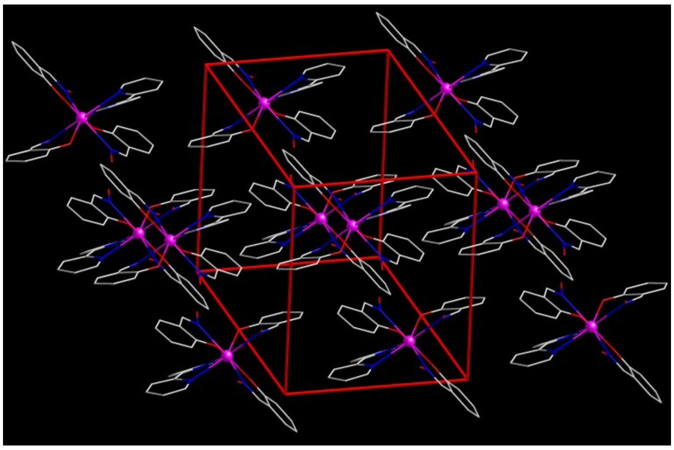

(a)

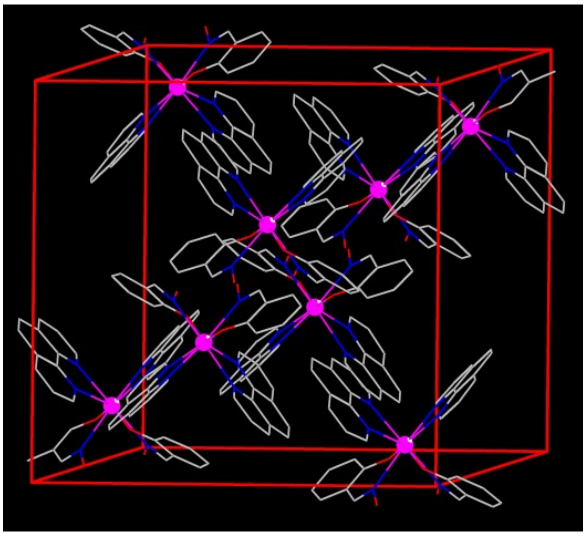

(b)

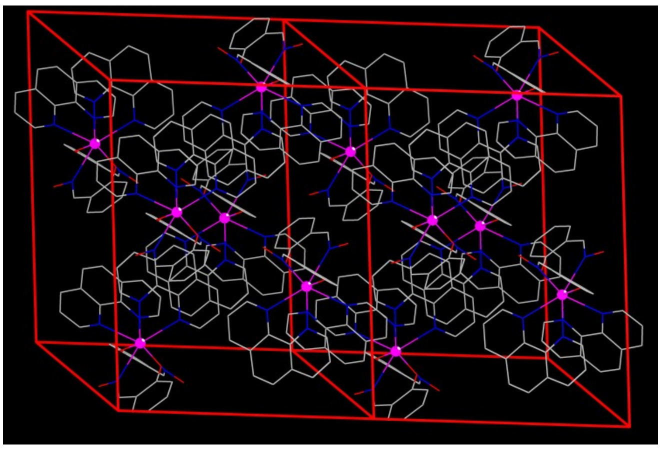

(c)

Fig. S2. Stacking structures of **1** (a) – **3** (c).

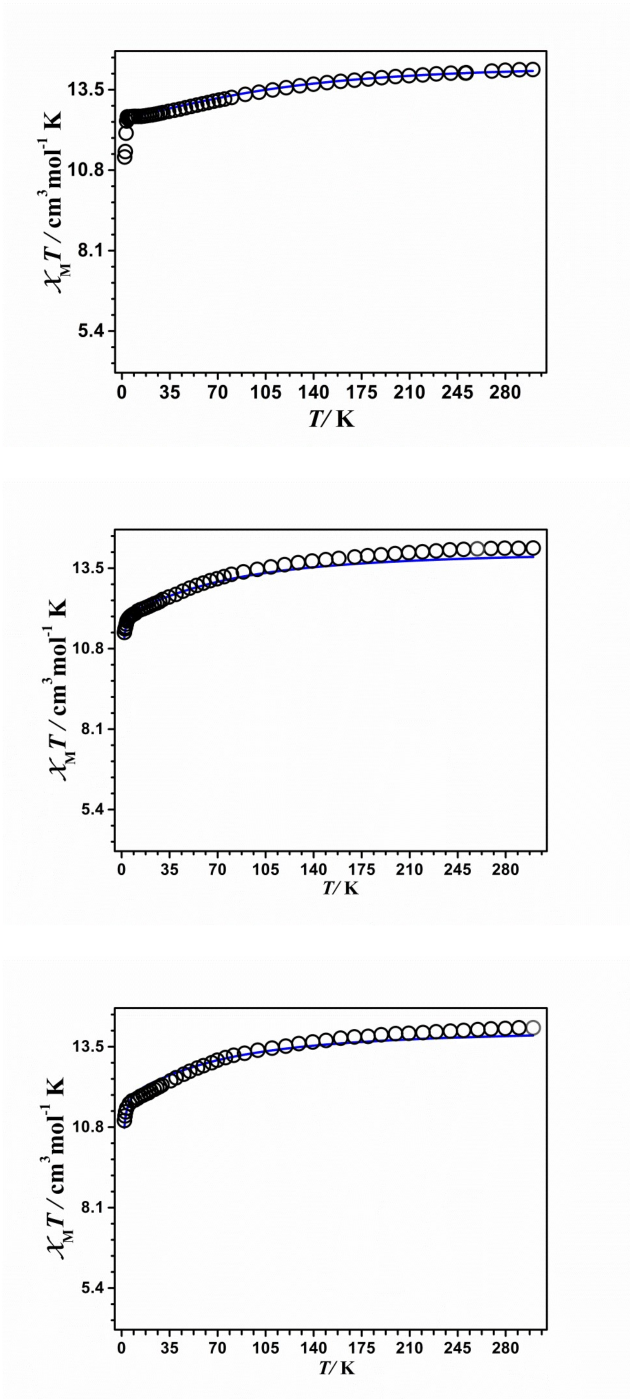

Fig. S3. Comparisons on the $\chi_\mathrm{M}T$–T curves between the theoretical calculation and experimental measurements for **1**–**3**.

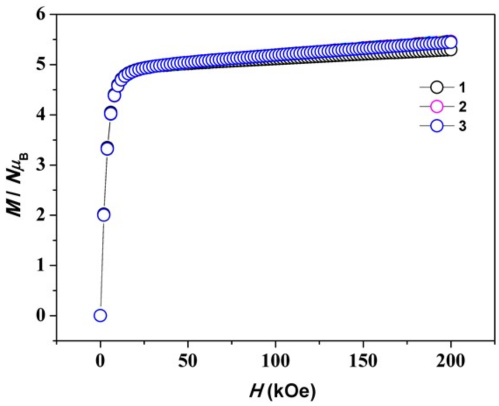

Fig. S4. The *M*–*H* curves for the theoretical calculation by *ab initio* at 2.0 K for **1**–**3**.

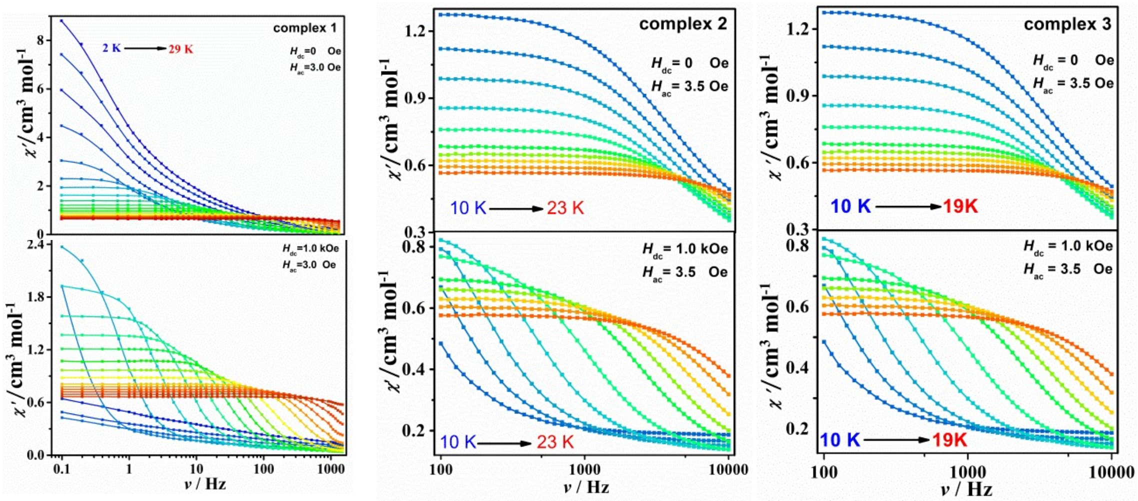

Fig. S5. Frequency dependence of the in-of-phase ac susceptibilities for **1–3**.

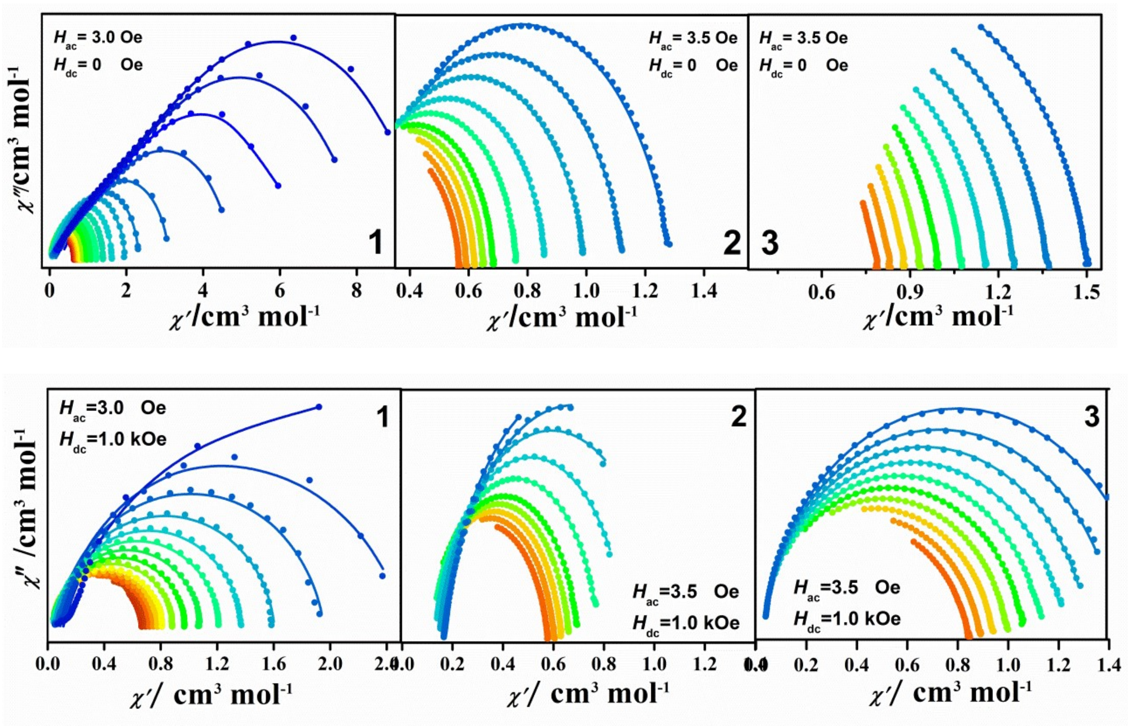

Fig. S6. Cole-Cole diagrams for **1**–**3** under zero and 1.0 kOe dc fields.

Table S8. The obtained fitting parameters for the Cole–Cole plots of **1** to the generalized Debye model under zero and 1.0 kOe dc fields.

T / K	zero dc field				Optimal 1.0 kOe field			
	χ_T (cm^3/mol)	χ_S (cm^3/mol)	τ / (s)	α	χ_T (cm^3/mol)	χ_S (cm^3/mol)	τ / (s)	α
29.0	0.64158	0.01260	4.23569E-5	0.03918	0.66517	0.04215	4.32263E-5	0.09031
28.5	0.68209	0.02491	5.41507E-5	0.03867				
28.0	0.69867	0.03381	7.10242E-5	0.03776	0.69623	0.03601	7.39467E-5	0.05907
27.5	0.70736	0.04757	9.25936E-5	0.03495				
27.0	0.71822	0.03118	1.13849E-4	0.02916	0.72218	0.01645	1.16208E-4	0.05705
26.5	0.73094	0.02933	1.43776E-4	0.02814				
26.0	0.75129	0.03793	1.82743E-4	0.02622	0.74913	0.01806	1.92162E-4	0.05352
25.0	0.77484	0.04014	2.83642E-4	0.02522	0.77903	0.03109	3.17093E-4	0.04794
24.0	0.81417	0.03932	4.18176E-4	0.03368	0.81174	0.0313	4.9049E-4	0.04631
22.0	0.88975	0.04476	8.17934E-4	0.03806	0.88541	0.0337	0.00103	0.04518
20.0	0.97829	0.05010	0.00138	0.04474	0.97218	0.03971	0.00188	0.04175
18.0	1.08860	0.05594	0.00222	0.05314	1.07885	0.04362	0.00322	0.04192
16.0	1.22975	0.06578	0.00364	0.07053	1.21724	0.04727	0.00576	0.04808
14.0	1.41407	0.07846	0.00623	0.09159	1.37559	0.05165	0.01088	0.05444
12.0	1.65839	0.10232	0.01142	0.11942	1.60348	0.06013	0.02271	0.06093

10.0	2.03723	0.12464	0.02382	0.17971	1.95183	0.07313	0.06056	0.0701
8.0	2.49722	0.15792	0.05536	0.26094	2.4887	0.09105	0.21801	0.09406
					3.82248	0.11034	1.79881	0.18111

Table S9. Calculated energy, *g* tensors, wave-functions and angles between the shortest Dy–O vector and the magnetic axis for the three lowest KDs of **1**–**3**

KDs	Energy (*K*)	g_x	g_y	g_z	θ (deg)	wave-function
1						
1	0.0	0.000	0.001	19.779	6.7	100%|±15/2>
2	344.6	0.087	0.140	16.563	22.4	79%|±11/2>+4%|±9/2>+12%|±7/2>+1%|±5/2>
3	467.7	1.180	1.493	13.898	48.2	2%|±15/2>+11%|±13/2>+26%|±11/2>+8%|±9/2>+ 27%|±7/2>+8%|±5/2>+13%|±3/2>+2%|±1/2>
2						
1	0.0	0.005	0.008	19.669	23.0	96%|±15/2>+4%|±11/2>
2	251.7	0.044	0.075	16.379	23.4	87%|±13/2>+1%|±11/2>+12%|±9/2>
3	433.2	0.632	0.889	12.979	24.4	2%|±15/2>+68%|±11/2>+1%|±9/2>+ 26%|±7/2>+1%|±5/2>+1%|±1/2>
3						
1	0.0	0.016	0.020	19.641	24.7	96%|±15/2>+4%|±11/2>
2	239.5	0.145	0.219	16.337	24.8	86%|±13/2>+14%|±9/2>
3	421.2	0.796	1.282	12.900	25.3	3%|±15/2>+68%|±11/2>+1%|±9/2>+27%|±7/2>+1%|±1/2>

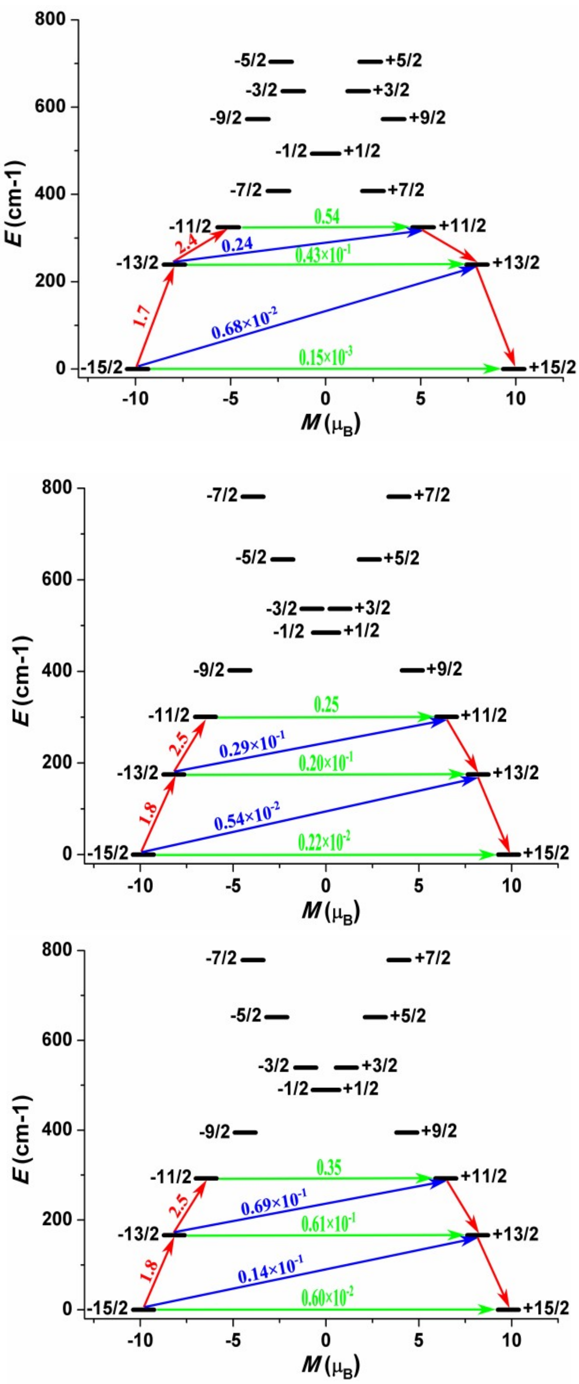

Fig. S7. *Ab initio* computed magnetization blocking barriers for **1**–**3**. The horizontal black lines represent the KDs as a function of their magnetic moment along the magnetic axis. The horizontal green lines within KDs correspond to diagonal quantum tunnelling of magnetization (QTM); the non-horizontal lines show the spin-phonon transition paths. The numbers at each arrow stand for the mean absolute value of the corresponding matrix element of transition magnetic moment.

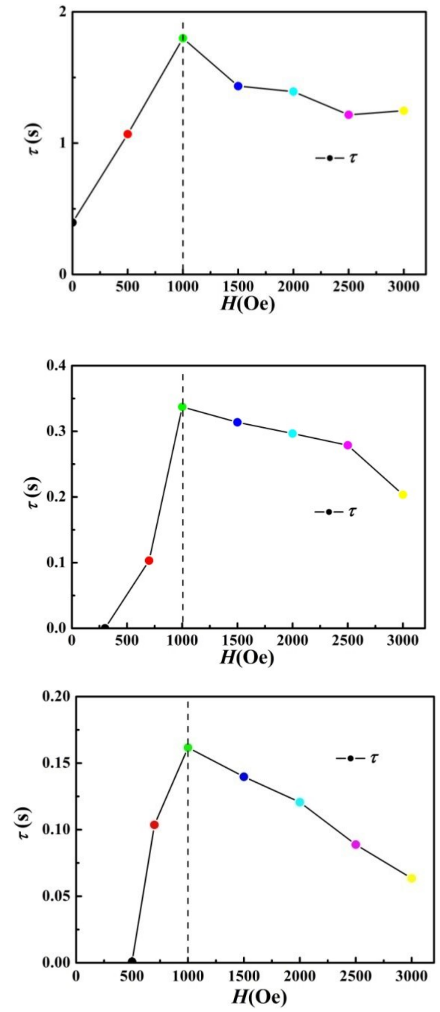

Fig. S8. Field dependence of the relaxation time for **1** (upper) – **3** (bottom) measured at 2.0 K.

Table S10. The obtained fitting parameters for the Cole–Cole plots of **2** to the generalized Debye model under zero and 1.0 kOe dc fields.

	zero dc field				Optimal 1.0 kOe field			
T / K	χ_T/ (cm^3/mol)	χ_S/ (cm^3/mol)	τ / (s)	α	χ_T / (cm^3/mol)	χ_S / (cm^3/mol)	τ / (s)	α
2								
10.0	1.28822	0.26813	4.10222E-5	0.14579	1.26355	0.16601	0.00376	0.10786
11.0	1.13159	0.23607	3.9738E-5	0.14434	1.15873	0.1536	0.00162	0.10554
13.0	0.99926	0.21558	3.77246E-5	0.12994	1.03793	0.14774	8.09022E-4	0.10376
15.0	0.86544	0.19304	3.37116E-5	0.10918	0.88743	0.13262	3.50176E-4	0.08527
17.0	0.76469	0.17643	2.75605E-5	0.08917	0.78083	0.12001	1.51813E-4	0.07803
19.0	0.68509	0.16018	1.98142E-5	0.06256	0.69749	0.10921	6.42747E-5	0.07686
20.0	0.65064	0.15348	1.60911E-5	0.05533	0.66295	0.10508	4.21404E-5	0.07832
21.0	0.62079	0.14558	1.27395E-5	0.05537	0.6321	0.10067	2.78766E-5	0.08263
22.0	0.59292	0.13979	9.95303E-6	0.05785	0.60422	0.09471	1.85832E-5	0.09021
23.0	0.56778	0.13586	7.75894E-6	0.06043	0.57847	0.08902	1.25596E-5	0.09812
3								
10.0	1.50502	0.24396	8.42339E-6	0.14054	1.57064	0.02089	4.12165E-4	0.07202
11.0	1.36906	0.22061	8.14823E-6	0.1382	1.43483	0.01568	2.48976E-4	0.07666
12.0	1.25494	0.19738	7.75329E-6	0.1336	1.32007	0.01268	1.56067E-4	0.07937
13.0	1.15865	0.18856	7.38376E-6	0.12632	1.22653	0.00842	1.00519E-4	0.08692
14.0	1.07621	0.15292	6.55727E-6	0.12604	1.14094	0.00581	6.52123E-5	0.09273
15.0	0.79677	0.08197	5.00792E-6	0.13415	1.06709	0.00542	4.26776E-5	0.09832
16.0	0.74781	0.03233	3.92396E-6	0.14484	1.00189	0.00669	2.78241E-5	0.10444
17.0	0.70507	0.01384	2.97642E-6	0.15132	0.94374	0.00755	1.81752E-5	0.11208
18.0	0.66651	0.00957	2.0013E-6	0.17227	0.89201	0.00771	1.18237E-5	0.12137
19.0	0.63228	0.00916	1.56501E-6	0.17891	0.84554	0.00828	7.53577E-6	0.13521